



Competent DNA binder pentagonal bipyramidal Fe(II) complex executed as a proficient catalyst for primary carbamates production from alcohols and urea



Malay Dolai^{a,*}, Sourav Pakrashy^a, Alope K. Ghosh^a, Surajit Biswas^{b,*}, Saugata Konar^{c,*}, Fatmah Ali Alasmay^d, Amani Salem Almalki^d, Md Ataul Islam^e

^a Department of Chemistry, Prabhat Kumar College, Contai, Purba Medinipur, West Bengal 721404, India

^b Department of Chemistry, University of Kalyani, Kalyani, Nadia, West Bengal 741235, India

^c Department of Chemistry, The Bhawanipur Education Society College, 5, Lala Lajpat Rai Sarani, Kolkata 700020, India

^d Department of Chemistry, College of Science, King Saud University, Riyadh 11451, Saudi Arabia

^e Division of Pharmacy and Optometry, School of Health Sciences, University of Manchester, United Kingdom

ARTICLE INFO

Article history:

Received 30 August 2022

Revised 15 November 2022

Accepted 16 November 2022

Available online 19 November 2022

Keywords:

Iron(II) complex

Pyrazole derived Schiff base ligand

X-ray crystal structure

DNA study

Catalysis

Primary carbamates production

ABSTRACT

The iron (II) complex, $[\text{Fe}(\text{H}_2\text{L})(\text{H}_2\text{O})_2](\text{ClO}_4)_2(\text{H}_2\text{O})$ (**1**) of Schiff base ligand H_2L [5-Methyl-1-H-pyrazole-3-carboxylic acid (1-pyridin-2-yl-ethylidene)-hydrazide] was prepared and structurally determined by X-ray crystal analysis. The complex **1** is being hepta-coordinated mononuclear system that adopts pentagonal bipyramidal geometry. Moreover, the calf thymus DNA (CT-DNA) interaction with **1** was carried out by proper bio-physical methods. The complex **1** was observed to interact with CT-DNA by intercalation binding mode and the binding constant of this interaction was calculated as $(1.5 \pm 0.06) \times 10^6 \text{ M}^{-1}$ and that was obtained from fluorimetric spectral titration. Again the complex **1** is very much effective in the catalytic reaction of primary carbamate synthesis. In this procedure alcohols and eco-friendly sustainable (**13:italic**) carbonylation/(**13:italic**) source urea were used for the synthesis of desired product. Both aromatic alcohols as well as aliphatic alcohols were efficiently proceeded through the catalytic reaction and produced medium to high yield (up to 94%) of carbamate products under mild reaction conditions. The catalytic mechanism was also supported by DFT studies.

© 2022 Elsevier B.V. All rights reserved.

1. Introduction

Pyrazole, a 5-membered heterocyclic ring, stands for a vital building block in organic chemistry as well as inorganic chemistry [1–3] and bioorganic, medicinal chemistry [4,5]. It attracted a lot of interest because of its simplicity in preparation and therapeutic potential as the foundation for cutting-edge medicinal applications. In the modern field of coordination chemistry, pyrazole-based hydrazones are of greater interest, and the variant substitutions in Schiff base-based pyrazole containing ligands [6–10] are most popular because of their structural flexibility and their major metal complexes exhibiting antitumor [11], antimicrobial [12], catalytic activities [13,14], anticancer [15] which is due to their chelating capability towards trace metal ions.

Moreover, iron is an essential component of both heme and non-heme enzymes, supporting a number of physiological functions including oxygen consumption, nerve conduction, electron

transfer, control of intracellular osmotic pressure, and DNA synthesis [16]. The iron (II) chelators are utilized as antitumor antibiotic and act as potential anticancer agents due to their efficiency to make oxidative damage in DNA, thus resulting of cancer cell's death [17]. Recently, there has been a lot of interest in the examination for the interaction between transition metals compound with DNA and these interactions [18,19] are covalent or intercalative interactions which may accelerate the gene mutations [20]. The major quantitative detection tools for the DNA in physico-chemical process are fluorescence and chemiluminescence [21,22]. Therefore, compound to DNA binding experiments are at the forefront of the research field, and are useful for further applications in DNA molecular drugs and novel chemotherapeutic probes [23]. Well known fact that the DNA interacts with drugs or substances in three non-covalent pathways; namely intercalation, groove binding and external interactions [24]. Fundamentally, the design and development of iron complexes with Schiff base ligands in coordination chemistry is of interest for this terrestrially abundant bio-compatible element.

* Corresponding authors.

E-mail addresses: dolaimalay@yahoo.in, dolaimalay@gmail.com (M. Dolai).

Carbamates are very crucial organic compounds frequently found in numerous medicines (like physostigmine, albendazole, flupirtine, and retigabine, etc.) [25–27], agro chemicals (as bactericides, herbicides, antiviral agents, and pesticides) [28–30], organic fine chemicals, cosmetics, polymer and biologically active compounds [31–33]. Carbamates are extremely beneficial for the production of peptides because they protect the amino groups of different amino acids [34–37]. Classically the said compounds are manufactured from alcohols and amines with the help of phosgene (COCl_2) as carbonyl source [38–40]. But this method is disadvantageous due to poor atom economy, elongated reaction hours, use of poisonous phosgene reagent, and noxious waste production [38–42]. In current scenario lots of attentions have been given to find out green pathways to facilitate the above reaction by using alternative carbonyl sources like *N*-acylbenzotriazoles [43], azides [44,45], 1,1,1-trichloromethyl formate (diphosgene) [46], carbonate esters [47], cyanate or isocyanate salts [48], isocyanides [49,50], 1,1-carbonyldiimidazole (CDI) [51,52], trichloroacetylchloride [53], dialkylazodicarboxylate [54], amides [55], and CO_2 in position of COCl_2 [56–59]. Although various optional carbonyl sources are utilized for the compound synthesis but the developed methodologies have the limitations of extreme reaction conditions, multi-step process, strong bases, expensive ligands and requirement of lethal metal-based catalysts. Now our concern is to build up an ecological, efficient and low-cost procedure for synthesis of carbamate products. The engagement of polyurea/urea as carbonyl sources for this derivative production is regarded as green and secure [60,61]. Beller et al. reported an environment friendly Lewis-acid FeBr_2 catalyst for primary carbamates synthesis via carbamoylation reaction from alcohols and urea [60]. Inaloo and his group has published very few publications where polyurea/urea was utilized as carbonyl sources for the manufacture of this derivatives [62,63]. M. Islam and his co-worker have published two different reports of primary carbamates production from urea and alcohol in presence of transition metal-based catalyst [62,64]. Recently A. H. Seikh and his group published a paper where an organo catalyst (graphene oxide) is used for this compound preparation under ambient conditions [65]. In the present study, the efforts have been constructed to synthesize iron complex as $[\text{Fe}(\text{H}_2\text{L})(\text{H}_2\text{O})_2](\text{ClO}_4)_2(\text{H}_2\text{O})$ (**1**) of the Schiff base ligand H_2L [5-Methyl-1-*H*-pyrazole-3-carboxylic acid (1-pyridin-2-yl-ethylidene)-hydrazide]. We have studied the interactions with double stranded DNA through fluorimetry and calorimetry and supported by molecular docking studies. Interestingly, we have also studied that iron complex **1** has efficient catalytic property for the preparation of primary carbamates by using urea and alcohols at 70 °C within 5 h of reaction.

2. Experimental section

2.1. Materials and methods

All chemicals were of reagent grade, purchased from commercial sources and used without further purification. $\text{Fe}(\text{ClO}_4)_2 \cdot x\text{H}_2\text{O}$ and 2,6-diacetylpyridine (97%) were purchased from Aldrich chemical company, USA and used without further purification.

Caution! Although we have not encountered any problem, it should be kept in mind that perchlorate compounds of metal ions are potentially explosive in the presence of organic ligands. Only a small amount of the material should be prepared and it should be handled with care.

2.2. Physical measurements

The Perkin-Elmer CHN analyzer 2400 at the Indian Association for the Cultivation of Science, Kolkata records. Elemental analysis

(carbon, hydrogen and nitrogen) of complex **1**. The electronic spectra of the complex were determined on a Hitachi model U-3501 spectrophotometer. IR spectra (KBr pellet, 500–4000 cm^{-1}) were carried out on a Perkin-Elmer model 883 infrared spectrophotometer. ^1H NMR spectra were recorded on a Bruker AMX-400 instrument using tetramethylsilane as internal standard.

2.3. Synthesis of the ligand (H_2L)

The ligand H_2L was synthesized according to our previously reported article [66] (Scheme 1). M.P. (°C) 138; Anal. Calc. for $\text{C}_{19}\text{H}_{21}\text{N}_9\text{O}_2$: C, 56.01; H, 5.20; N, 30.94. Found: C, 55.97; H, 5.17; N, 30.89%. IR (KBr, cm^{-1}): 1528 (py $\nu_{\text{C}=\text{N}}$), 1442 (pz $\nu_{\text{C}=\text{N}}$), 1682 ($\nu_{\text{C}=\text{O}}$), 1081 (pz $\nu_{\text{N}=\text{N}}$), 3271 ($\nu_{\text{N}-\text{H}}$), *m/z* 407 (M^+ , 100%). ^1H NMR (in d_6 -DMSO, δ): 13.13 (s, 1NH, ring Pz), 10.29 (s, 1H, ring Pz), 8.08 (d, $J = 7.2$ Hz, 2H, ring Py), 7.89 (t, $J = 7.8$ Hz, 1H, ring Py), 6.52 (s, 1H, aliphatic NH), 2.46 (s, 6H, $-\text{CH}_3$).

2.4. Synthesis of $[\text{Fe}(\text{H}_2\text{L})(\text{H}_2\text{O})_2](\text{ClO}_4)_2(\text{H}_2\text{O})$ (**1**)

$\text{Fe}(\text{ClO}_4)_2 \cdot x\text{H}_2\text{O}$ (1 mmol, 0.254 g) was reacted with the ligand H_2L [66] (1 mmol, 0.407 g) in methanol solvent nearly at 60 °C in refluxing mode. The mixture was taken in 1:1 molar ratio. The solution turned brown after 2 h continuous stirring.

The resulting solution was kept aside untouched for a week then brown crystals of **1** (Scheme 1) suitable for single crystal diffraction, were deposited. Then the crystals were washed and collected by filtration with cold methanol and dried in air. (Yield: 58.5%). Anal. Calc. for $\text{C}_{19}\text{H}_{25}\text{Cl}_2\text{FeN}_9\text{O}_{13}$ (MW 714.23): C, 31.92; H, 3.50; N, 17.64. Found: C, 31.89; H, 3.48; N, 17.67%. IR (KBr, cm^{-1}): 1037 (s), 1474 (s), 1664 (s), 3200 (m).

2.5. Crystallographic measurements

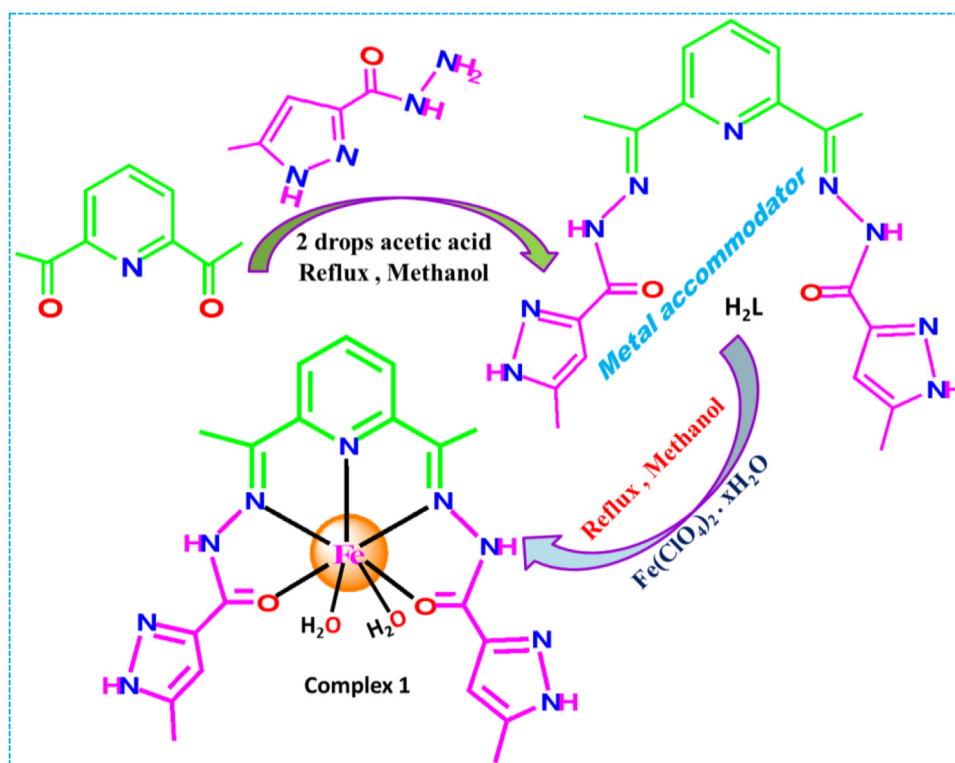
The data collection for complex **1** were made using Bruker SMART APEX CCD as a detector equipped with graphite monochromated $\text{Mo K}\alpha$ radiation ($\lambda = 0.71073$ Å) source in φ and ω scan mode. Cell parameters refinement and data reduction were carried out using Bruker SMART [67] and Bruker SAINT softwares for the complex. In **1**, structure was solved by conventional direct methods and refined by full-matrix least square methods using F^2 data. SHELXS-97 and SHELXL-97 programs [68] were used for structure solution and refinement, respectively. In **1**, all non-hydrogen atoms were refined as anisotropic by Fourier full matrix least squares F^2 . Hydrogen atoms on nitrogen and oxygen atoms were found from a Fourier difference map and were allowed to refine while all other hydrogen atoms were placed in calculated positions. There are two non-coordinated water oxygen atoms are disordered throughout two positions with occupancy 0.5. Selected crystal data for **1** is given in Table S1 and selected metrical parameters of the complex **1** are given in Table S2.

2.6. DNA binding measurements

The details procedure is described in ESI file.

2.7. Fluorescence spectral titration with DNA

The fluorescence spectral titrations [69,70] were performed as previous reports. The steady-state fluorescence measurements were performed on a Shimadzu RF-5301 PC unit (Shimadzu Corporation, Kyoto, Japan) in fluorescence free quartz cuvettes of 1 cm path length. The excitation wavelength for complex **1** was 350 nm. All measurements were performed keeping an excitation and emission band pass of 5 nm. The sample temperature was maintained at 298.15 ± 1.0 K using an Eyla Uni Cool U55 water bath (Tokyo Rikakikai Co. Ltd., Tokyo, Japan).



Scheme 1. Schematic diagram for synthesis of ligand (H_2L) and **1**.

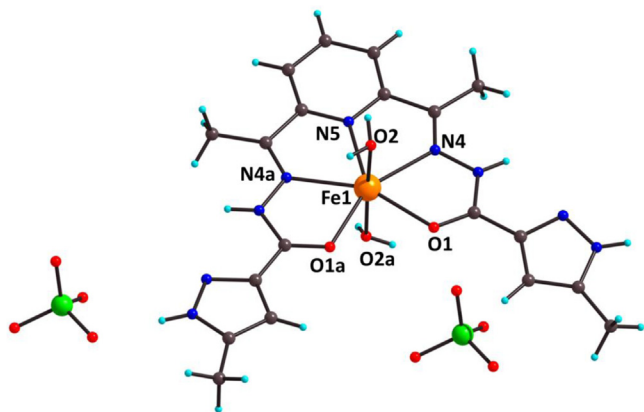


Fig. 1. Molecular view of **1** with partially labeled atoms (disorder water molecule is omitted for clarity).

3. Result and discussion

3.1. Structural description of $[Fe(H_2L)(H_2O)_2](ClO_4)_2(H_2O)$ (**1**)

The single crystal X-ray analysis shows that complex **1** is crystallized in *monoclinic* system with space group $C12/c1$. The asymmetric unit is iron (II) mononuclear with the ligand H_2L (Scheme 1), acted as a pentadentate chelator (Fig. 1). However, central metal iron (II) is coordinated by three nitrogen atoms: one pyridyl nitrogen atom (N5), two azomethine nitrogen atoms (N4 and N4a) and two hydrazolyl oxygen atoms (namely O1 and O1a) from ligand and spanning itself in the equatorial plane. The central atom iron is further coordinated by two apical water molecules (O2 and O2a) and attained pentagonal bipyramidal geometry with N_3O_4 chromophore using a ligand molecule. The important bond distances and angles data (Table S2) are in well corrob-

orated with the reported similar hepta-coordinated Mn(II) complexes [22,71]. The M – N (pyridine) bond distance of complex **1** is Fe(1)–N(5) = 2.248(3) Å and other azomethine and hydrazone bonds are in good agreement with previous report [71]. The axial water molecules coordinating the central metal ion is a little diverged from the linear arrangement and the angle is O(2)–Fe(1)–O(2)a = 174.11(9)°.

The complex **1** is stabilized through the intermolecular hydrogen bonding network (Fig. 2). There are several types of intermolecular hydrogen bonding interactions, remaining between (a) hydrogen atom of coordinated water molecule and nitrogen atom of pyrazole ring of another unit (H2A...N2 = 2.21(6)Å), (b) oxygen atom of perchlorate ion and hydrogen atom of coordinated water molecule (H2B...O3 = 2.16(5)Å) and (c) perchlorate oxygen atom and hydrogen atom of pyrazole ring nitrogen (H1...O4 = 2.16(4)Å and H1...O5 = 2.46(4)Å) forming 1D network along crystallographic *b* axis (Fig. 2a). The 1D network further extended to 2D framework in crystallographic *ac* plane (Fig. 2b). The details of the H-bonding interactions are given in Table S3.

3.2. DNA binding tests

3.2.1. Fluorescence titrations

Fluorescence spectral titration study is considered as the most widespread tool for estimating the binding of target drug agents with nucleic acids (DNA or RNA). Generally, changes in the fluorescence and/or the peak position shifting are the usual things when a drug molecule interacts with DNA making a complex [72]. The degree of interaction is very much related with the changes in the peak position.

The emission titration of **1** with DNA was observed at 430–600 nm wavelength zone upon excitation at 350 nm. The emission titration studies were performed by titrating at static concentration of **1** (20 μM) with increasing amount of DNA. However, a 2.0-fold increase in the emission intensity of **1** was observed (with

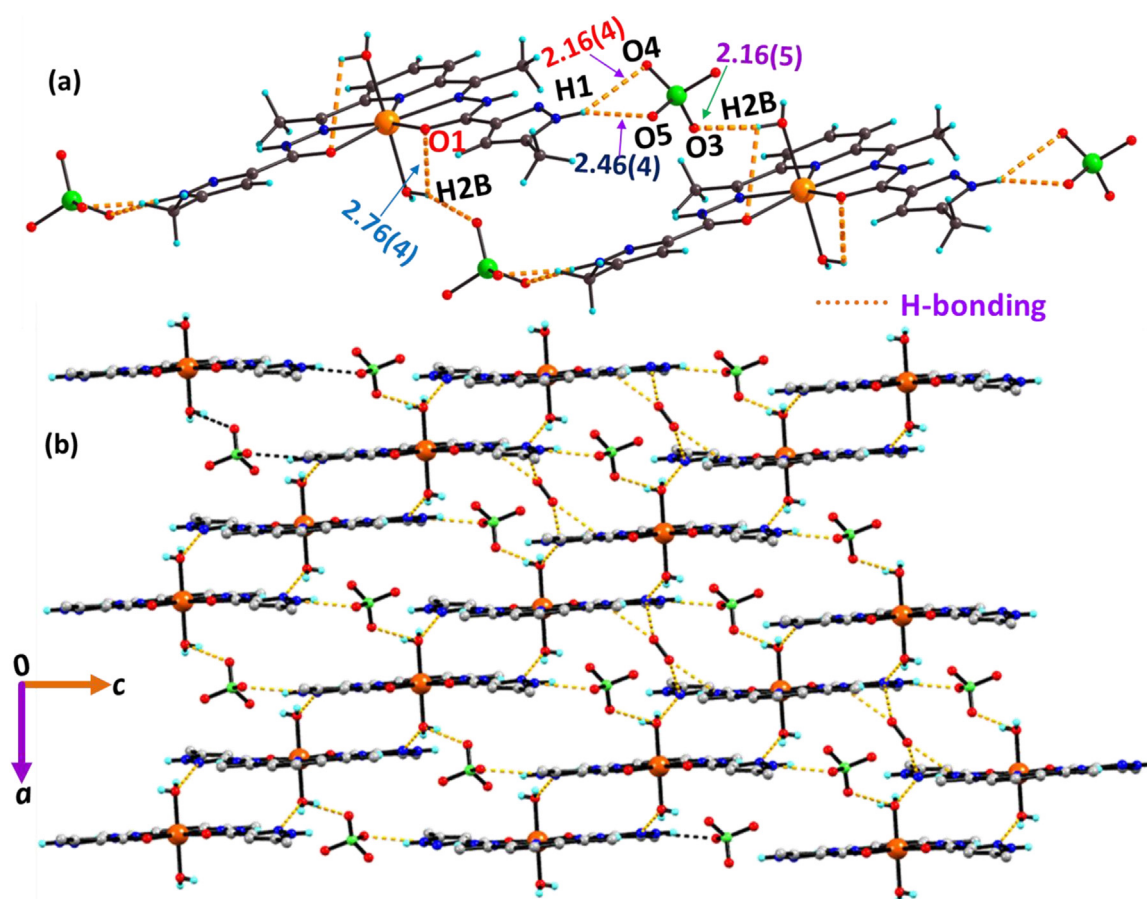


Fig. 2. (a) The hydrogen bonded 1D network along crystallographic *b* axis, and (b) 2D H-bonding structural design in crystallographic *ac* plane for **1**.

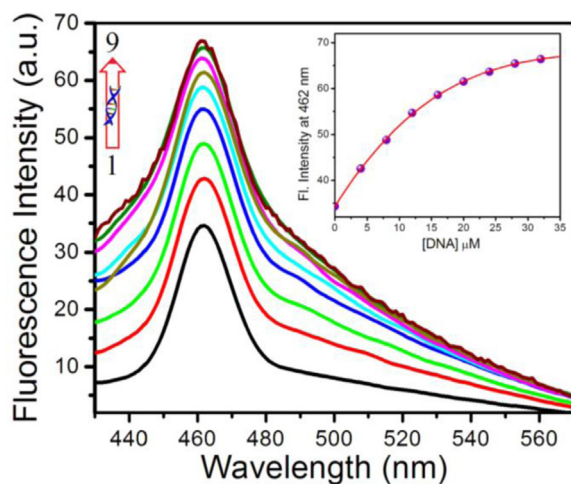


Fig. 3. Fluorescence titration profile of **1** ($20 \mu\text{M}$) with incremental amount of CT DNA [$0\text{--}32 \mu\text{M}$]; inset: plot of emission maxima at 462 nm vs [DNA]. Excitation wavelength was 350 nm .

$0\text{--}32 \mu\text{M}$ DNA) at the fluorescence maxima at 462 nm (Fig. 3). This increase in the intensity upon addition to DNA proposed a strong binding of **1** with DNA.

Benesi–Hildebrand (B–H) plots [73] were used to calculate the apparent equilibrium constant (K) for **1**–DNA binding. B–H plot was obtained by using the spectra from emission titrations data. From B–H plot, the apparent equilibrium constant value K_{BH} was calculated as $(1.5 \pm 0.06) \times 10^6 \text{ M}^{-1}$.

On the other hand, the binding stoichiometry of **1** with DNA was calculated from Job's plot [72]. The plot of (ΔF), emission intensity changes at 462 nm (λ_{max}) versus mole fraction were drawn for **1** and the cutting point (χ) was calculated to be 0.497 , and the stoichiometry was detected as 1.06 (Fig. S6).

3.2.2. Competitive dye displacement studies with ethidium bromide

Ethidium bromide was used as emission probe that exhibited strong emission with interaction of DNA due to its solid intercalation in between adjacent DNA base pairs [71–73]. The method was showing that this strong emission may be decreased as quench by drug agent which could intercalate with DNA by entering and replacing EB from its DNA binding sites. The emission spectral titration of EB bind to DNA and with complex **1** ($0\text{--}78 \mu\text{M}$) is shown in Fig. 4.

The adding of **1** to DNA pre-treated with EB lead to almost 48.6% decreased in emission intensity. The notable dropping in emission intensity of EB–DNA gave a solid proof for intercalation of the complex **1** into the double helixed DNA by displacing the bound EB.

3.2.3. Molecular docking studies

Molecular docking study is well recognized tool in drug discovery field for experiencing the binding mode and interaction between drug molecule as complex **1** and double helix DNA [71]. From docking study (Fig. 5), it is shown that the **1** was well seated in between the helix of the DNA. The docking conformation exhibits that the pyrazole ring (pz), Fe atom of **1** were intensely fixed into the DNA strand through intercalation mode and there are hydrogen bonding interactions and π ...methyl interactions viz. $\text{O}_{\text{Thymine}} \cdots \text{H}_{\text{pz}}$, $\text{O}_{\text{phosphate}} \cdots \text{H}_{\text{pz}}$ and $\pi_{\text{phosphate}} \cdots (\text{methyl})_{\text{pz}}$ and

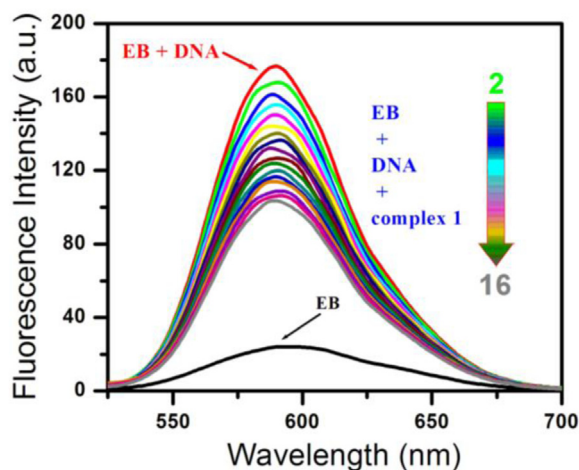
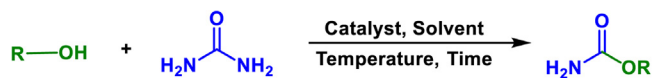


Fig. 4. Fluorescence emission spectra of the competition between the EB–DNA complex (λ_{exc} : 350 nm) and **1**. C_{EB} = 1.91 μM and C_{DNA} : 20 μM , $C_{\text{complex 1}}$: 0.0–78 μM .



Scheme 2. Catalytic preparation of primary carbamates from urea and alcohols.

very few electrostatic bindings (Fig. S2). The docking score was gained at $-10.7 \text{ kcal}\cdot\text{mole}^{-1}$ as binding energy. Hence, docking simulation exhibited that interaction between **1** and DNA was the energetically preferable binding path and that was evidenced by ethidium bromide displacement assay experiment.

3.3. Catalytic production of primary carbamates using urea and alcohols

After achieving very good interaction of iron complex **1** with DNA, we have tried another application of the complex in the field of catalysis. The complex **1** showed an excellent catalytic activity in synthesis of industrially important primary carbamates from environmentally benign urea and alcohols (Scheme 2).

In the beginning, the catalytic reaction was started by taking urea (5 mmol) and benzyl alcohol (8 mmol) in acetonitrile solvent at 70 °C in presence of complex **1** (0.01 mmol). To our delight, the reaction afforded 61% of benzyl carbamate product after 5 h of reaction (Table 1, entry 1). Despite of using excess alcohol only one side nucleophilic substitution reaction was proceeds, so corresponding dibenzyl carbonate product formation is inhibited. The same reaction was performed in the absence of complex **1**; only 29% of desired product was obtained in 5h of reaction (Table 1, entry 2). Therefore, our synthesized iron complex **1** has definitely a strong catalytic activity in this carbamate formation reaction. All these initial data encourage us to optimize the catalytic conditions of the reaction. Solvent is the very important parameter for any catalytic reaction, so we carried out the above reaction in presence of various solvents (Table 1, entries 3–11). Although all solvents except water and *n*-dibutylether (*n*-Bu₂O) gave us moderate to high yield of benzyl carbamate product; 1,4-dioxane was the most suitable solvent for the reaction that produced 80% yield of the product (Table 1, entry 9). The reaction was monitored in the absence of any solvent but that did not create any hopeful result (Table 1, entry 12). Then the model reaction was explored in the presence of various iron metal precursors as catalyst instead of complex **1** (Table 1, entries 13–17). Only moderate amount of desired product yield was obtained. Reaction temperature is another key factor for any catalytic reaction. So, we started optimization of reaction temperature afterward (Table 1, entries 18, 19). When the reaction temperature was reduced from 70 °C to 60 °C, the yield percentage of the product also decreased due to diminution number of fruitful collisions between substrate and active site of catalyst (Table 1, entry 18). Again, with increasing reaction temperature the product yield did not alter very much from 80% (Table 1, entry 19).

Finally, the effect of catalyst amount on the reaction was checked at 70 °C. Fig. 6 clearly shows that with increment of catalyst loading (up to 0.02 mmol) also increased the percentage of desired product yield. Further enhancement of catalyst amount (from 0.02 to 0.025) did not produce any extra amount of preferred product. So, 0.02 mmol catalyst is enough for the maximum yield of the product (92%).

After completion of optimization of the catalytic reaction conditions we went for substrate tolerance for the reaction. Different types of alcohols such as benzyl alcohols, aromatic alcohols and aliphatic alcohols smoothly went through the catalytic reaction and

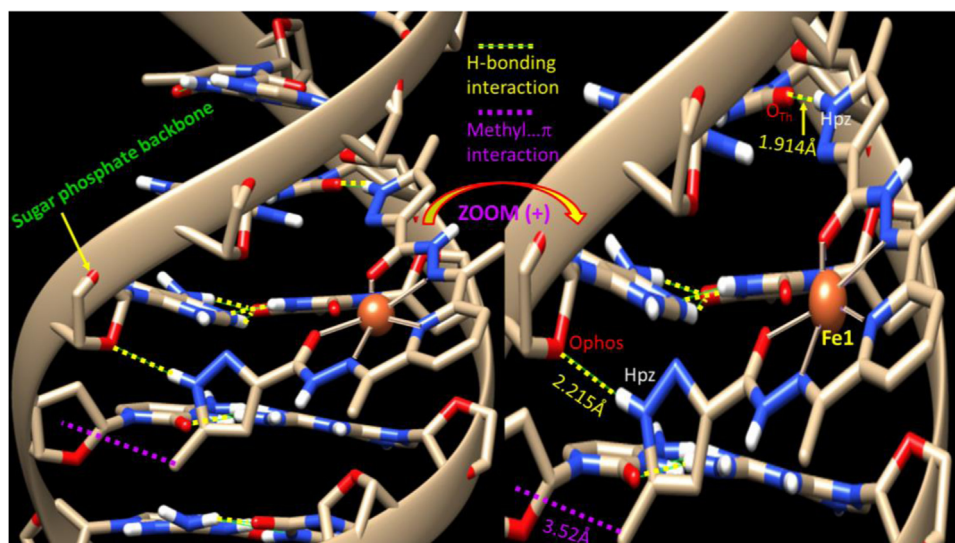
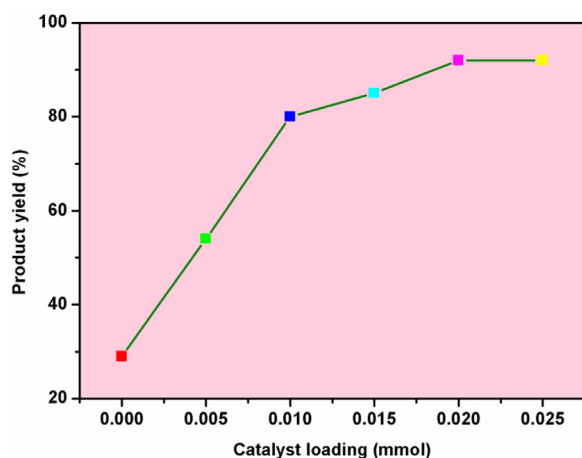


Fig. 5. Capped sticks model viewed into the intercalation of DNA by **1**. There is colored grey, white, red, blue and orange, (C, H, O, N and Fe, respectively). The important hydrogen bonding interactions between different sections of the **1**–DNA complex are illustrated with yellow dashed lines.

Table 1
Optimization table for catalytic benzyl carbamate synthesis reaction^a.

Entry	Solvent	Catalyst	Temperature (°C)	% yield of benzyl carbamate ^b
1	Acetonitrile	1	70	61
2	Acetonitrile	-	70	29
3	Dichloromethane	1	70	53
4	Chloroform	1	70	56
5	Benzene	1	70	68
6	Toluene	1	70	70
7	DMSO	1	70	71
8	DMF	1	70	73
9	1,4-Dioxane	1	70	80
10	Water	1	70	Trace
11	n-Bu ₂ O	1	70	Trace
12	No solvent	1	70	Trace
13	1,4-Dioxane	Fe(ClO ₄) ₂ .xH ₂ O	70	52
14	1,4-Dioxane	FeCl ₂	70	54
15	1,4-Dioxane	Fe(NO ₃) ₃	70	49
16	1,4-Dioxane	FeBr ₂	70	55
17	1,4-Dioxane	Fe(OAc) ₂	70	50
18	1,4-Dioxane	1	60	66
19	1,4-Dioxane	1	80	82

^a Reaction conditions: Urea (5 mmol), benzyl alcohol (8 mmol), catalyst (0.01 mmol), 5 h.^b isolated yield.**Fig. 6.** Effect of catalyst loading on benzyl carbamate formation reaction [condition: Urea (5 mmol), benzyl alcohol (8 mmol), catalyst (0.01 mmol), 70 °C, 5 h].

produced moderate to high yield of corresponding carbamate products (Table 2). Benzyl alcohol reacts with urea and formed 92% isolated yield of benzyl carbamate after 5 h of reaction (Table 2, entry 1). 4-methoxybenzyl alcohol produced slightly greater amount of corresponding carbamate (94%) due to the presence of electron donating methoxy group (Table 2, entry 2). Whereas benzyl alcohol having moderate electron withdrawing group (-Br) produced lesser amount of carbamate product (82%) in 5.5 h. Again, more reduction of product yield (64%) was observed when strong electron withdrawing group containing 4-nitro benzyl alcohol was taken part in the reaction (Table 2, entry 4). From phenol, we got 78% yield of phenyl carbamate (Table 2, entry 5). While electron donating group containing 4-methyl and 4-methoxy phenol yielded better quantity of desired products (Table 2, entries 6, 7). Again 4-nitro phenol gave only 59% of carbamate product due to the presence of strong electron withdrawing nitro group in para position (Table 2, entry 8). Additionally aliphatic alcohols (such as propyl alcohol, butyl alcohol and isopropyl alcohol) produced high yield (>83%) of respective carbamate products via this catalysis reaction (Table 2, entries 9–11) relatively in lower reaction duration (4 h).

A comparison between previously published methodologies with our developed protocol for the synthesis of benzyl carbamate

from urea and benzyl alcohol is sum up in Table 3. Almost all previous reports required high temperature (>120 °C) for the production of high yield benzyl carbamate^{42a, 44b, 45a}. Only one report produced high percentage of benzyl carbamate (96.7%) at mild temperature (80 °C)^{45b}. Our developed protocol synthesized high yield of the said product (92%) at relatively lower temperature (i.e. 70 °C) after 5h of reaction.

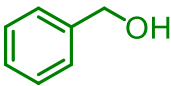
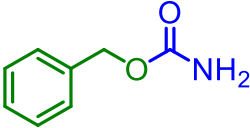
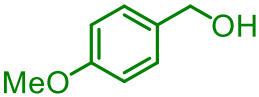
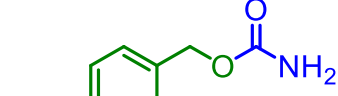
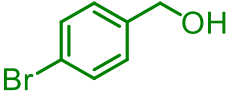
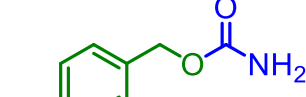
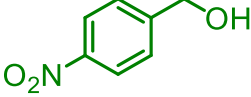
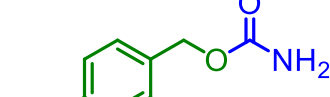
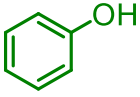
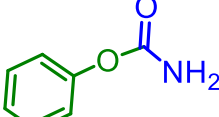
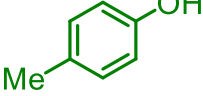
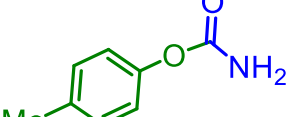
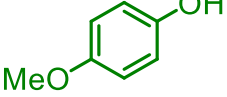
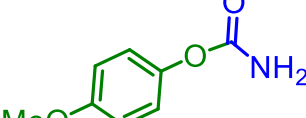
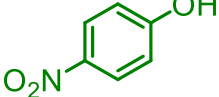
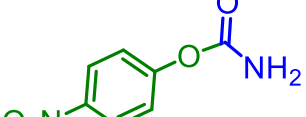

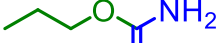
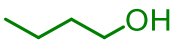
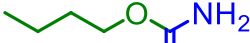
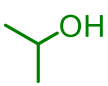
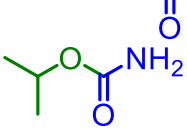
3.4. A probable reaction mechanism for catalytic synthesis of carbamate

The single crystal structural view of complex **1** exhibited that there was a hepta-coordinated Fe(II) center which is able to coordinate to urea through the O-atoms of urea that is the key leading force for the enriched catalytic carbamate synthesis.

To realize the mechanism of the carbamate synthesis reaction between benzyl alcohol (ROH) and urea catalyzed by complex **1**, the theoretical calculations were accomplished using DFT/LanL2Dz for full catalytic observations (theoretical calculation details are in ESI). From former results [60–65] and the experimental outcomes, it was compared that urea molecule is initiated by the interface of the iron atom of complex **1** by the oxygen donor atom of urea (structure-I) which can take responsibility to initiate the said catalytic reactions. The respective energies for all intermediates involve in catalytic reaction of ROH and urea in attendance of complex **1** is presented in Fig. 7. The catalytic site of complex **1** is primarily considered as zero for the whole calculations. Firstly, the complex **1** removed its one neutral water molecule and simultaneous coordination of Fe(II) ion with oxygen atom (⁴Fe(II)...O_{urea} = 3.58Å) from urea and was grown the electrophilic character at the carbonyl carbon in urea which was tending to the formation of intermediate-I (-17.03 × 10³ kcal mol⁻¹) [62]. Further, the catalytic reaction was continued forward, in where the very reactive nucleophilic such as benzyl alcohol (ROH) tended at the carbonyl carbon of urea as electron lacking center to form an intermediate -II (structure II) with respective energy of -20.61 × 10³ kcal mol⁻¹ [65].

Then, the intermediate-II was simultaneously, undergoing an intramolecular proton transfer from protonated benzyl alcohol (ROH) to the amine group of urea and form an intermediate-III (-20.64 × 10³ kcal mol⁻¹) which was the iron coordinated ammonium intermediate. Both intermediate -II and -III were in equilibrium by their relative energy. In the last moment of the catalysis,

Table 2
Substrate scope for primary carbamates formation reaction^a.

Entry	Alcohol	Products	Time (h)	Yield (%) ^b
1			5	92
2			5	94
3			5.5	82
4			6	64
5			5	78
6			5	80
7			5	81
8			6	59
9			4	86
10			4	91
11			4	84

^a Reaction conditions: Urea (5 mmol), alcohols (8 mmol), catalyst (0.02 mmol), 1,4-dioxane (6 ml), 70 °C.^b isolated yield.**Table 3**
Comparison table for catalytic synthesis of benzyl carbamate with previous reports.

Entry	Catalyst	Reaction conditions	Yield (%)	Ref.
1	FeBr ₂	urea (0.5 mmol), benzyl alcohol (0.75 mmol), catalyst (0.01 mmol), 1,4-dioxane (1 mL), 150 °C, 6 h	92	60a
2	MNP-Fe ₃ O ₄	urea (2 mmol), benzylalcohol (1 mmol), [ChCl][ZnCl ₂] (3 mL), catalyst (10 mol %), 130 °C, 6 h	90	63b
3	Fe ^{II} (Anthra-Merf)	benzyl alcohol (3 mmol), urea (2 mmol), catalyst (0.020 g), 1,4-dioxane (3.5 mL), 120 °C, 6.5 h	97	63a
4	Cu-NPs@TzTa-POP	benzyl alcohol (5 mmol), urea (4 mmol), catalyst (20 mg), 1,4-dioxane (4 ml), 80 °C, 4 h	96.7	64b
5	Complex 1	urea (5 mmol), benzyl alcohol (8 mmol), catalyst (0.02 mmol), 1,4-dioxane (6 ml), 70 °C, 5 h	92	This work

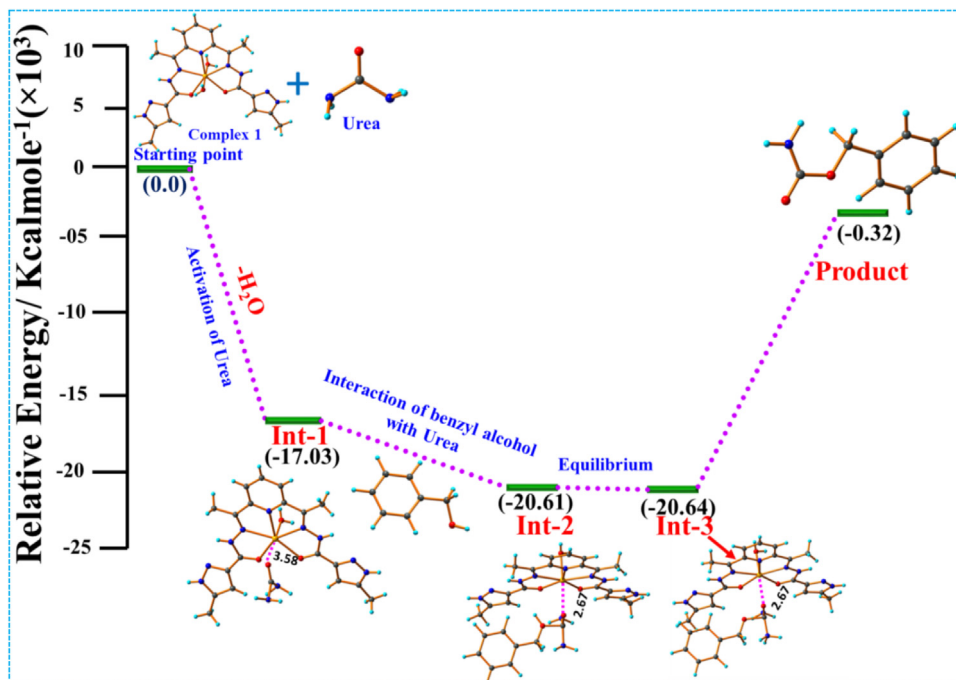


Fig. 7. Relative free energy frame for complex 1 catalyzed carbamate synthesis from urea and benzyl alcohol (ROH).

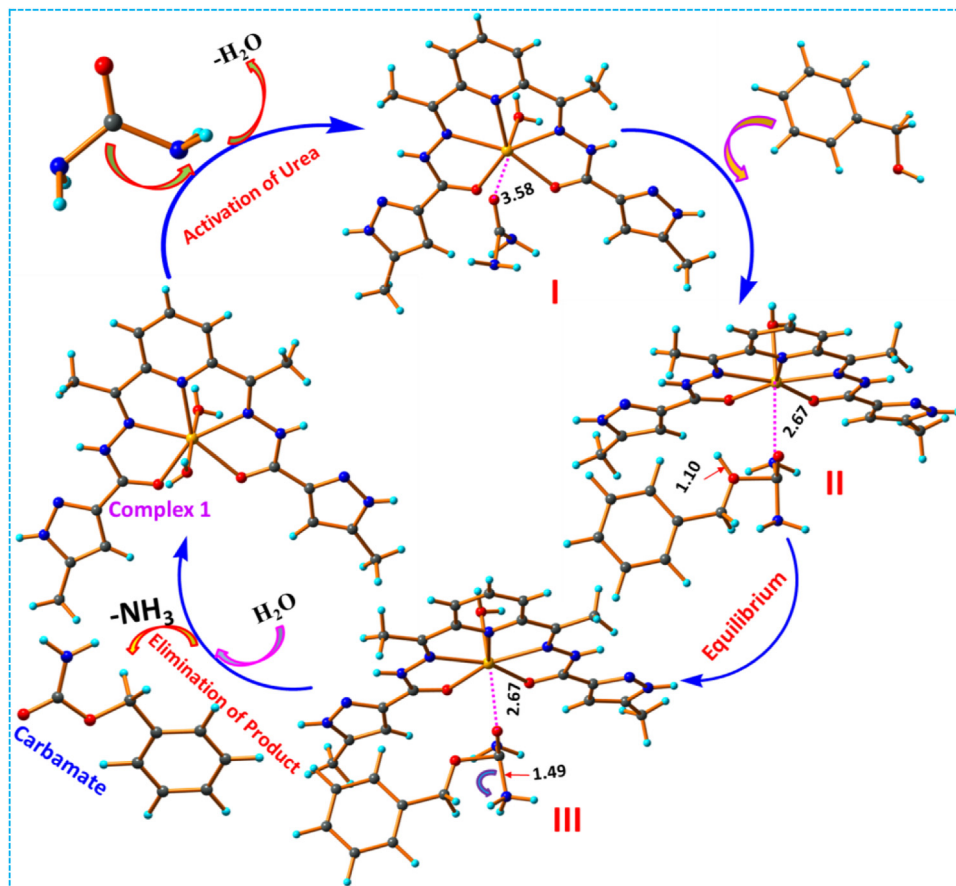


Fig. 8. Probable mechanism for the carbamate synthesis by the reaction of urea with benzyl alcohol catalyzed by complex 1 (cited bond lengths are in angstrom).

the ammonia molecule was removed from intermediate –III after auto-decomposition of the ammonium compound by breaking of oxygen to iron co-ordinate bond ($d(\text{Fe(II)}\dots\text{O}_{\text{urea}}) = 2.67\text{\AA}$) and released the final product carbamate. After releasing of carbamate, the Fe(II) was coordinated with one water molecule to give re-birth of complex **1**, which is the main criteria of a catalyst that remains intact and unaffected after completion of catalytic reaction cycle.

The above-mentioned major steps were compiled with three intermediates between start the journey of catalysis and final product. The respective energies attained for Int-1, Int-2, Int-3 and product were -17.03×10^3 , -20.61×10^3 , -20.64×10^3 and -0.32×10^3 kcal mol⁻¹, respectively.

The probable mechanism is structured (Fig. 8) upon the evidenced from experimental results and theoretical simulations for the catalytic reaction of urea and benzyl alcohol to form benzyl carbamate (BC). The above-mentioned mechanism is the good agreement with previous reported articles [60–65].

4. Conclusion

In conclusion, the Schiff base based iron complex $[\text{Fe}(\text{H}_2\text{L})(\text{H}_2\text{O})_2](\text{ClO}_4)_2(\text{H}_2\text{O})$ (ligand H_2L [5-Methyl-1-H-pyrazole-3-carboxylic acid (1-pyridin-2-yl-ethylidene)-hydrazide]) was synthesized and structurally characterized through single crystal XRD. The structural analysis showed that the mononuclear iron center in complex, adopted the pentagonal bipyramidal geometry. Then the interactions of this complex with double stranded DNA were studied by fluorometric processes and the binding constant of this interaction was about $(1.5 \pm 0.06) \times 10^6$ M⁻¹. The EtBr displacement studies also showed that the interaction was partial intercalation. The mentioned interaction was supported by molecular docking studies and that is favored by energy about -10.7 kcal·mole⁻¹. Moreover, the said complex **1** showed its efficiency as a catalyst for the conversion of urea and alcohols to primary carbamates at 70 °C within 6 h of reaction. Both aliphatic and aromatic alcohols had been efficiently undergone the catalytic path and produced very high isolated yield (up to 94%) of desired product. Then the probable catalytic mechanism of the catalytic conversion was well corroborated with literatures and framed on the basis of theoretical calculations.

Credit authors statement

All authors are done their own parts of the manuscripts with their utmost sincerity.

Declaration of Competing Interest

There is no conflict of interest to declare

Data Availability

The data that has been used is confidential.

Acknowledgements

M.D gratefully acknowledges and thanks the I-STEM/catalytic grant/acad-08/2021-2022 for the research support. S.K. thanks The Bhawanipur Education Society College, Kolkata, India for financial support [Project No. BESC/PC/2019-2020/SC1/02]. Authors also acknowledge to U. Saha for her constant supports for the interpretation of biological studies. F. A. Alasmay and A. S. Almalki are thankful to the researcher supporting project (RSP-2021/259), King Saud University, Riyadh, Saudi Arabia.

Supplementary materials

CCDC 2052192 contains the supplementary crystallographic data for **1**. These data can be obtained free of charge via <http://www.ccdc.cam.ac.uk/conts/retrieving.html>, or from the Cambridge Crystallographic Data Centre, 12 Union Road, Cambridge CB2 1EZ, UK; fax: (+44) 1223-336-033; or e-mail: deposit@ccdc.cam.ac.uk.

Supplementary material associated with this article can be found, in the online version, at doi:10.1016/j.molstruc.2022.134584.

References

- [1] Y.R. Girish, K.S.S. Kumar, H.S. Manasa, S. Shashikanth, ZnO: an ecofriendly, green nano-catalyst for the synthesis of pyrazole derivatives under aqueous media, *J. Chin. Chem. Soc.* 61 (2014) 1175–1179, doi:10.1002/jccs.201400170.
- [2] T.R. Swaroop, K.S. Sharath Kumar, M. Palanivelu, S. Chaitanya, K.S. Rangappa, A catalyst-free green protocol for the synthesis of pyranopyrazoles using room temperature ionic liquid choline chloride-urea, *J. Heterocycl. Chem.* 51 (2014) 1866–1870, doi:10.1002/jhet.1864.
- [3] S. Sengupta, S. Ganguly, A. Goswami, S. Bala, S. Bhattacharya, R. Mondal, Construction of Co(II) coordination polymers comprising of helical units using a flexible pyrazole based ligand, *CrystEngComm* 14 (2012) 7428–7437, doi:10.1039/C2CE25256B.
- [4] H.R. Puneeth, H. Ananda, K.S.S. Kumar, K.S. Rangappa, A.C. Sharada, Synthesis and antiproliferative studies of curcumin pyrazole derivatives, *Med. Chem. Res.* 25 (2016) 1842–1851.
- [5] H. Ananda, K.S. Sharath Kumar, M. Nishana, M. Hegde, M. Srivastava, R. Byregowda, B. Choudhary, S.C. Raghavan, K.S. Rangappa, Regioselective synthesis and biological studies of novel 1-aryl-3, 5-bis (het) aryl pyrazole derivatives as potential antiproliferative agents, *Mol. Cell. Biochem.* 426 (2017) 149–160, doi:10.1007/s11010-016-2887-7.
- [6] K. Karrouchi, S. Radi, Y. Ramli, J. Taoufik, Y.N. Mabkhot, F.A. Al-aizari, M. Ansar, Synthesis and pharmacological activities of pyrazole derivatives: a review, *Molecules* 23 (2018) 134, doi:10.3390/molecules23010134.
- [7] F.E. Bennani, L. Doudach, Y. Cherrah, Y. Ramli, K. Karrouchi, M. Ansar, M.E.A. Faouzi, Overview of recent developments of pyrazole derivatives as an anticancer agent in different cell line, *Bioorg. Chem.* 97 (2020) 103470.
- [8] K. Chkirate, K. Karrouchi, N. Dege, N.K. Sebbar, A. Ejjoummany, S. Radi, N.N. Adarsh, A. Talbaoui, M. Ferbinteanu, E.M. Essassi, Y. Garcia, Co(II) and Zn(II) pyrazolyl-benzimidazole complexes with remarkable antibacterial activity, *New J. Chem.* 44 (2020) 2210–2221.
- [9] K. Chkirate, S. Fettach, K. Karrouchi, N.K. Sebbar, E.M. Essassi, J.T. Magued, S. Radi, M.E.A. Faouzi, N.N. Adarsh, Y. Garcia, Novel Co(II) and Cu(II) coordination complexes constructed from pyrazole-acetamide: effect of hydrogen bonding on the self assembly process and antioxidant activity, *J. Inorg. Biochem.* 191 (2019) 21–28.
- [10] K. Chkirate, K. Karrouchi, H. Chakchak, J.T. Mague, S. Radi, N.N. Adarsh, W. Li, A. Talbaoui, E.M. Essassi, Y. Garcia, Coordination complexes constructed from pyrazole-acetamide and pyrazole-quinoxaline: effect of hydrogen bonding on the self-assembly process and antibacterial activity, *RSC Adv.* 12 (2022) 5324.
- [11] H. Dai, S. Ge, J. Guo, S. Chen, M. Huang, J. Yang, S. Sun, Y. Ling, Y. Shi, Development of novel bis-pyrazole derivatives as antitumor agents with potent apoptosis induction effects and DNA damage, *Eur. J. Med. Chem.* 143 (2018) 1066–1076, doi:10.1016/j.ejmech.2017.11.098.
- [12] S.M. Anush, B. Vishalakshi, B. Kalluraya, N. Manju, Synthesis of pyrazole-based Schiff bases of Chitosan: evaluation of antimicrobial activity, *Int. J. Biol. Macromol.* 119 (2018) 446–452, doi:10.1016/j.ijbiomac.2018.07.129.
- [13] J. Yang, Pyrazole-3-carboxylates assisted N-heterocyclic carbene palladium complexes: synthesis, characterization, and catalytic activities towards arylation of azoles with arylsulfonyl hydrazides, *Appl. Organomet. Chem.* 34 (2020) e5450, doi:10.1002/aoc.5450.
- [14] N. Onishi, R. Kanega, E. Fujita, Y. Himeda, Cover picture: carbon dioxide hydrogenation and formic acid dehydrogenation catalyzed by iridium complexes bearing pyridyl-pyrazole ligands: effect of an electron-donating substituent on the pyrazole ring on the catalytic activity and durability (adv. synth. catal. 2/2019), *Adv. Synth. Catal.* 361 (2019) 220, doi:10.1002/adsc.201801550.
- [15] A. Balbi, M. Anzaldi, C. Macciò, C. Aiello, M. Mazzei, R. Gangemi, P. Castagnola, M. Miele, C. Rosano, M. Viale, Synthesis and biological evaluation of novel pyrazole derivatives with anticancer activity, *Eur. J. Med. Chem.* 46 (2011) 5293–5309, doi:10.1016/j.ejmech.2011.08.014.
- [16] T. Ma, X. Zhao, Y. Matsuo, J. Song, R. Zhao, M. Faheem, M. Chen, Y. Zhang, Y. Tian, G. Zhu, Fluorescein-based fluorescent porous aromatic framework for Fe³⁺ detection with high sensitivity, *J. Mater. Chem. C* 7 (2019) 2327–2332, doi:10.1039/C8TC06288A.
- [17] R.M. Burger, Nature of Activated Bleomycin BT - Metal-Oxo and Metal-Peroxo Species in Catalytic Oxidations, in: B. Meunier (Ed.), Springer Berlin Heidelberg, Berlin, Heidelberg, 2000: pp. 287–303. 10.1007/3-540-46592-8_10.
- [18] C.J. Dhanaraj, I.U. Hassan, J. Johnson, J. Joseph, R.S. Joseyphus, Synthesis, spectral characterization, DNA interaction, anticancer and molecular docking studies on some transition metal complexes with bidentate ligand, *J. Photochem. Photobiol. B Biol* 162 (2016) 115–124, doi:10.1016/j.jphotobiol.2016.06.032.
- [19] M. Lazou, A. Tarushi, P. Gritzapis, G. Psomas, Transition metal complexes with a novel guanine-based (E)-2-(2-(pyridin-2-ylmethylene)hydrazinyl)quinazolin-

- 4(3H)-one: Synthesis, characterization, interaction with DNA and albumins and antioxidant activity, *J. Inorg. Biochem.* 206 (2020) 111019, doi:10.1016/j.jinorgbio.2020.111019.
- [20] C.V. Kumar, E.H. Asuncion, DNA binding studies and site selective fluorescence sensitization of an anthryl probe, *J. Am. Chem. Soc.* 115 (1993) 8547–8553, doi:10.1021/ja00072a004.
- [21] F. Anam, A. Abbas, K.M. Lo, Zia-ur-Rehman, S. Hameed, M.M. Naseer, Homologous 1,3,5-triarylpyrazolines: synthesis, CH $\cdots\pi$ interactions guided self-assembly and effect of alkyloxy chain length on DNA binding properties, *New J. Chem.* 38 (2014) 5617–5625, doi:10.1039/C4NJ00938J.
- [22] U. Saha, B. Das, M. Dolai, R.J. Butcher, G. Suresh Kumar, Adaptable DNA-interactive probe proficient at selective turn-on sensing for Al $^{3+}$: insight from the crystal structure, photophysical studies, and molecular logic gate, *ACS Omega* 5 (2020) 18411–18423, doi:10.1021/acsomega.0c02226.
- [23] M. Dolai, U. Saha, G.S. Kumar, M. Ali, Amidooxime-based mononuclear Mn(II) complexes: synthesis, characterization, and studies on DNA binding and nuclease activity, *ChemistrySelect* 3 (2018) 6935–6941, doi:10.1002/slct.201801298.
- [24] U. Saha, M. Dolai, G.S. Kumar, Targeting nucleic acid with a bioactive fluorophore: Insights from spectroscopic and calorimetric studies, *J. Mol. Struct.* 1220 (2020) 128690, doi:10.1016/j.molstruc.2020.128690.
- [25] B.H. Peters, H.S. Levin, Effects of physostigmine and lecithin on memory in Alzheimer disease, *Ann. Neurol.* 6 (1979) 219–221, doi:10.1002/ana.410060307.
- [26] A.G. Saimot, A.C. Cremieux, J.M. Hay, A. Meulemans, M.D. Giovanangeli, B. Delaitre, J.P. Coulaud, Albendazole as a potential treatment for human hydatidosis, *Lancet* 322 (1983) 652–656, doi:10.1016/S0140-6736(83)92533-3.
- [27] A.D. Wickenden, W. Yu, A. Zou, T. Jegla, P.K. Wagoner, Retigabine, a novel anti-convulsant, enhances activation of KCNQ2/Q3 potassium channels, *Mol. Pharmacol.* 58 (2000) 591–600, doi:10.1124/mol.58.3.591.
- [28] N. Haque, S. Biswas, P. Basu, I. Haque Biswas, R. Khatun, A. Khan, S.M. Islam, Triazinetriamine-derived porous organic polymer-supported copper nanoparticles (Cu-NPs@TzTa-POP): an efficient catalyst for the synthesis of N-methylated products via CO $_2$ fixation and primary carbamates from alcohols and urea, *New J. Chem.* 44 (2020) 15446–15458, doi:10.1039/D0NJ02798G.
- [29] J.A. Ocampo, J.M. Barea, Effect of carbamate herbicides on VA mycorrhizal infection and plant growth, *Plant Soil* 85 (1985) 375–383, doi:10.1007/BF02220192.
- [30] J.S. Van Dyk, B. Pletschke, Review on the use of enzymes for the detection of organochlorine, organophosphate and carbamate pesticides in the environment, *Chemosphere* 82 (2011) 291–307, doi:10.1016/j.chemosphere.2010.10.033.
- [31] M. Suzuki, A. Ii, T. Saegusa, Multibranching polymerization: palladium-catalyzed ring-opening polymerization of cyclic carbamate to produce hyperbranched dendritic polyamine, *Macromolecules* 25 (1992) 7071–7072, doi:10.1021/ma00051a055.
- [32] B. Husár, R. Liska, Vinyl carbonates, vinyl carbamates, and related monomers: synthesis, polymerization, and application, *Chem. Soc. Rev.* 41 (2012) 2395–2405, doi:10.1039/C1CS15232G.
- [33] O. Kreye, H. Mutlu, M.A.R. Meier, Sustainable routes to polyurethane precursors, *Green Chem.* 15 (2013) 1431–1455, doi:10.1039/C3GC40440D.
- [34] T.W. Turney, A. Patti, W. Gates, U. Shaheen, S. Kulasegaram, Formation of glycerol carbonate from glycerol and urea catalysed by metal monoglycerolates, *Green Chem.* 15 (2013) 1925–1931, doi:10.1039/C3GC37028C.
- [35] W. Fan, Y. Queneau, F. Popowycz, HMF in multicomponent reactions: utilization of 5-hydroxymethylfurfural (HMF) in the Biginelli reaction, *Green Chem.* 20 (2018) 485–492, doi:10.1039/C7GC03425C.
- [36] Frontmatter, Greene's Protective Groups in Organic Synthesis. (2006) i–xxviii. 10.1002/9780470053485.fmatter.
- [37] U. Jacquemard, V. Bénéteau, M. Lefoix, S. Routier, J.Y. Mérour, G. Coudert, Mild and selective deprotection of carbamates with Bu $_4$ NF, *Tetrahedron* 60 (2004) 10039–10047, doi:10.1016/j.tet.2004.07.071.
- [38] P.L. Spargo, Phosgenations - A Handbook By Livius Cotarca and Heiner Eckert. Wiley-VCH: Weinheim. 2004. 656 pp. £217.50. ISBN 3-527-29823-1, *Org. Process Res. Dev.* 8 (2004) 1085–1086, doi:10.1021/op049865d.
- [39] C. Pubill-Ulldemolins, A. Bonet, C. Bo, H. Gulyás, E. Fernández, Activation of diboron reagents with brønsted bases and alcohols: an experimental and theoretical perspective of the organocatalytic boron conjugate addition reaction, *Chem. Eur. J.* 18 (2012) 1121–1126, doi:10.1002/chem.201102209.
- [40] M. Carafa, F. Iannone, V. Mele, E. Quaranta, Solventless selective phosgene-free N-carboxylation of N-heteroaromatics (pyrrole, indole, carbazole) under mild conditions, *Green Chem.* 14 (2012) 3377–3385, doi:10.1039/C2GC36103E.
- [41] S.T. Hobson, R.P. Casillas, R.A. Richieri, R.N. Nishimura, R.H. Weisbart, R. Tuttle, G.T. Reynolds, M.H. Parseghian, Development of an acute, short-term exposure model for phosgene, *Toxicol. Mech. Methods* 29 (2019) 604–615, doi:10.1080/15376516.2019.1636170.
- [42] S.A. Cucinelli, E. Arsenal, Review of the toxicity of long-term phosgene exposure, *Arch. Environ. Health: Int. J.* 28 (1974) 272–275, doi:10.1080/00039896.1974.10666485.
- [43] A.S. Singh, D. Kumar, N. Mishra, V.K. Tiwari, An efficient one-pot synthesis of N,N'-disubstituted ureas and carbamates from N-acylbenzotriazoles, *RSC Adv.* 6 (2016) 84512–84522, doi:10.1039/C6RA14131E.
- [44] C.R. Sagandira, P. Watts, Synthesis of amines, carbamates and amides by multi-step continuous flow synthesis, *Eur. J. Org. Chem.* 2017 (2017) 6554–6565, doi:10.1002/ejoc.201700906.
- [45] L. Ren, N. Jiao, PdCl $_2$ catalyzed efficient assembly of organic azides, CO, and alcohols under mild conditions: a direct approach to synthesize carbamates, *Chem. Commun.* 50 (2014) 3706–3709, doi:10.1039/C4CC00538D.
- [46] K. Kurita, T. Matsumura, Y. Iwakura, Trichloromethyl chloroformate. Reaction with amines, amino acids, and amino alcohols, *J. Org. Chem.* 41 (1976) 2070–2071, doi:10.1021/jo00873a053.
- [47] M. Carafa, E. Quaranta, Synthesis of organic carbamates without using phosgene: carbonylation of amines with carbonic acid diesters, *Mini Rev. Org. Chem.* 6 (2009) 168–183, doi:10.2174/157019309788922720.
- [48] Y.H. Jung, J.D. Kim, One-pot synthesis of cinnamylamines with various protecting groups from cinnamyl ethers, *Arch. Pharm. Res.* 24 (2001) 371, doi:10.1007/BF02975178.
- [49] X.B. Bu, Z. Wang, Y.H. Wang, T. Jiang, L. Zhang, Y.L. Zhao, Rhodium-catalyzed oxidative coupling reaction of isocyanides with alcohols or amines and molecular oxygen as oxygen source: synthesis of carbamates and ureas, *Eur. J. Org. Chem.* 2017 (2017) 1132–1138, doi:10.1002/ejoc.201601484.
- [50] G.C. Tron, Isocyanide chemistry. Applications in synthesis and material science. Edited by Valentine G. Nenajdenko, *Angew. Chem. Int. Ed.* 51 (2012) 12659, doi:10.1002/anie.201209150.
- [51] M. Lanzillotto, L. Konner, F. Lamaty, J. Martinez, E. Colacino, Mechanochemical 1,1'-carbonyldiimidazole-mediated synthesis of carbamates, *ACS Sustain. Chem. Eng.* 3 (2015) 2882–2889, doi:10.1021/acssuschemeng.5b00819.
- [52] J.A. Grzyb, M. Shen, C. Yoshina-Ishii, W. Chi, R.S. Brown, R.A. Batey, Carbamoylimidazolium and thiocarbamoylimidazolium salts: novel reagents for the synthesis of ureas, thioureas, carbamates, thiocarbamates and amides, *Tetrahedron* 61 (2005) 7153–7175, doi:10.1016/j.tet.2005.05.056.
- [53] J.H. Wynne, S.D. Jensen, A.W. Snow, Facile one-pot synthesis of S-alkyl thiocarbamates, *J. Org. Chem.* 68 (2003) 3733–3735, doi:10.1021/jo026813i.
- [54] M. Usman, Z.H. Ren, Y.Y. Wang, Z.H. Guan, Copper-catalyzed carbonylation of anilines by diisopropyl azodicarboxylate for the synthesis of carbamates, *RSC Adv.* 6 (2016) 107542–107546, doi:10.1039/C6RA22108D.
- [55] P. Liu, Z. Wang, X. Hu, Highly efficient synthesis of ureas and carbamates from amides by iodobenzene-induced Hofmann rearrangement, *Eur. J. Org. Chem.* 2012 (2012) 1994–2000, doi:10.1002/ejoc.201101784.
- [56] M. Feroci, M. Orsini, L. Rossi, G. Sotgiu, A. Inesi, Electrochemically promoted C–N bond formation from amines and CO $_2$ in ionic liquid BMIm–BF $_4$: synthesis of carbamates, *J. Org. Chem.* 72 (2007) 200–203, doi:10.1021/jo061997c.
- [57] A. Ion, C. Van Doorslaer, V. Parvulescu, P. Jacobs, D. De Vos, Green synthesis of carbamates from CO $_2$, amines and alcohols, *Green Chem.* 10 (2008) 111–116, doi:10.1039/B711197E.
- [58] D. Chaturvedi, S. Ray, Versatile use of carbon dioxide in the synthesis of carbamates, *Monatsh. Chem./Chem. Mon.* 137 (2006) 127–145, doi:10.1007/s00706-005-0423-7.
- [59] N. Germain, I. Müller, M. Hanauer, R.A. Paciello, R. Baumann, O. Trapp, T. Schaub, Synthesis of industrially relevant carbamates towards isocyanates using carbon dioxide and organotin(IV) alkoxides, *ChemSusChem* 9 (2016) 1586–1590, doi:10.1002/cssc.201600580.
- [60] M. Peña-López, H. Neumann, M. Beller, Iron-catalyzed reaction of urea with alcohols and amines: a safe alternative for the synthesis of primary carbamates, *ChemSusChem* 9 (2016) 2233–2238, doi:10.1002/cssc.201600587.
- [61] P. Wang, Y. Ma, S. Liu, F. Zhou, B. Yang, Y. Deng, N-Substituted carbamate synthesis using urea as carbonyl source over TiO $_2$ -Cr $_2$ O $_3$ /SiO $_2$ catalyst, *Green Chem.* 17 (2015) 3964–3971, doi:10.1039/C5GC01007A.
- [62] I. Dindarloo Inaloo, S. Majnooni, Ureas as safe carbonyl sources for the synthesis of carbamates with deep eutectic solvents (DESs) as efficient and recyclable solvent/catalyst systems, *New J. Chem.* 42 (2018) 13249–13255, doi:10.1039/C8NJ02624F.
- [63] I.D. Inaloo, S. Majnooni, M. Esmaeilpour, Superparamagnetic Fe $_3$ O $_4$ nanoparticles in a deep eutectic solvent: an efficient and recyclable catalytic system for the synthesis of primary carbamates and monosubstituted ureas, *Eur. J. Org. Chem.* 2018 (2018) 3481–3488, doi:10.1002/ejoc.201800581.
- [64] P. Basu, T.K. Dey, A. Ghosh, S. Biswas, A. Khan, S.M. Islam, An efficient one-pot synthesis of industrially valuable primary organic carbamates and N-substituted ureas by a reusable Merrifield anchored iron(ii)-anthra catalyst [Fe II (Anthra-Merf)] using urea as a sustainable carbonylation source, *New J. Chem.* 44 (2020) 2630–2643, doi:10.1039/C9NJ05675K.
- [65] S.M. Wabaidur, M.R. Siddiqui, A.H. Seikh, Graphene oxide (GO) as sustainable heterogeneous carbocatalyst for synthesis of organic carbamates using urea and alcohols under mild reaction conditions, *Chemistryselect* 6 (2021) 13461–13467, doi:10.1002/slct.202103635.
- [66] S. Konar, A. Jana, K. Das, S. Ray, S. Chatterjee, J.A. Golen, A.L. Rheingold, S.K. Kar, Synthesis, crystal structure, spectroscopic and photoluminescence studies of manganese(II), cobalt(II), cadmium(II), zinc(II) and copper(II) complexes with a pyrazole derived Schiff base ligand, *Polyhedron* 30 (2011) 2801–2808, doi:10.1016/j.poly.2011.08.018.
- [67] SMART (V 5.628), SAINT (V 6.45a), SMART (V 5.628), SAINT (V 6.45a), XPREP, SHELXTL, Bruker AXS Inc., Madison, Wisconsin, USA, 2004.
- [68] G.M. Sheldrick, Crystal paper reference, *Acta Crystallogr. Sect. C Struct. Chem.* C71 (2015) 3–8.
- [69] U. Saha, A. Yasmeen Khan, S. Bhuiya, S. Das, G. Fiorillo, P. Lombardi, G. Suresh Kumar, Targeting human telomeric DNA quadruplex with novel berberubine derivatives: insights from spectroscopic and docking studies, *J. Biomol. Struct. Dyn.* 37 (2019) 1375–1389, doi:10.1080/07391102.2018.1459319.
- [70] U. Saha, M. Dolai, G.S. Kumar, R.J. Butcher, S. Konar, New DNA-interactive manganese(II) complex of amidooxime: crystal structure, DFT calculation, biophysical and molecular docking studies, *J. Chem. Eng. Data* 65 (2020) 5393–5404, doi:10.1021/acs.jced.0c00529.

- [71] H.A. Benesi, J.H. Hildebrand, A spectrophotometric investigation of the interaction of iodine with aromatic hydrocarbons, *J. Am. Chem. Soc.* 71 (1949) 2703–2707, doi:[10.1021/ja01176a030](https://doi.org/10.1021/ja01176a030).
- [72] A.Y. Khan, U. Saha, G. Fiorillo, P. Lombardi, G.S. Kumar, Calorimetric insights into the interaction of novel berberrubine derivatives with human telomeric g-quadruplex dna sequence, *J. Therm. Anal. Calorim.* 132 (2018) 623–630, doi:[10.1007/s10973-018-6960-1](https://doi.org/10.1007/s10973-018-6960-1).
- [73] U. Saha, M. Dolai, G.Suresh Kumar, Adaptable sensor for employing fluorometric detection of methanol molecules: theoretical aspects and DNA binding studies, *New J. Chem.* 43 (2019) 8982–8992, doi:[10.1039/C9NJ01018A](https://doi.org/10.1039/C9NJ01018A).